Green Chemistry

Accepted Manuscript

ROYAL SOCIETY OF CHEMISTRY

www.rsc.org/greenchem

Production of Biodiesel and Hydrogen from Plant Oil Catalyzed by Magnetic Carbon-Supported Nickel and Sodium Silicate

Fan Zhang[2, 3], Xue-Hua Wu[2, 3], Min Yao[2], Zhen Fang[1, 2*], Yi-Tong Wang[2, 3]

[1] Biomass Group, College of Engineering, Nanjing Agricultural University, 40 Dianjiangtai Road, Nanjing, Jiangsu 210031, China

[2] Chinese Academy of Sciences, Biomass Group, Key Laboratory of Tropical Plant Resources and Sustainable Use, Xishuangbanna Tropical Botanical Garden, 88 Xuefulu, Kunming, Yunnan Province, 650223, China

[3] University of Chinese Academy of Sciences, 19A Yuquan Road, Beijing, 100049, China

[4] Faculty of Science, Kunming University of Science and Technology, Kunming, Yunnan Province, 650223, China

*Author for correspondence
Zhen Fang (zhen.fang@mail.mcgill.ca)

Emails:
Zhang, fan: zhangfan226@126.com
Wu, xue-hua: wuxuehua78@163.com
Yao, min: 876384129@qq.com
Wang, yi-tong: 1192627817@qq.com

Revised for Green Chemistry

Feb. 2016

Abstract

A novel magnetic carbon-based nickel and sodium silicate catalyst (Na_2SiO_3@Ni/C) was prepared by precipitation of $Ni(OH)_2$ on bamboo powders, pyrolysis and loading of Na_2SiO_3 for biodiesel and hydrogen co-production. The catalyst had strong magnetism (magnetic saturation, Ms of 15.7 Am^2/kg) from Ni and basicity (3.18 mmol/g) from Na_2SiO_3 for magnetic separation and biodiesel production. In the presence of Na_2SiO_3@Ni/C, biodiesel yield of 98.1% was achieved from soybean oil under the best conditions (9/1 methanol/oil molar ratio, 7 wt% catalyst, 65 °C for 100 min) optimized by single-factor experiments. The catalyst was cycled 4 times with biodiesel yield > 93%, but the yield dropped to 80.9% with 85.3% catalyst recovery rate at the fifth cycle. The deactivated catalyst after 5 cycles catalyzed the hydrothermal gasification of biodiesel by-product (crude glycerol) at 350 °C for 5 min with gasification rate of 80.1% and 82.7% H_2 purity. The role of Ni is to catalyze H_2 production while Na_2SiO_3 is to absorb CO_2 to achieve high H_2 concentration. After gasification, the structure of Ni/C changed slightly and can be still cycled to load Na_2SiO_3 for biodiesel production and subsequent gasification.

Keywords: Biodiesel; Magnetic catalyst; Crude glycerol; Hydrothermal gasification; Hydrogen.

1. Introduction

Utilization of renewable and clean fuels is an attractive option for reducing greenhouse gas emissions and improving energy security,[1] many countries have been directed towards the exploitation of alternative biofuels,[2] such as bioethanol[3], biodiesel[4] and biogas[5]. Biodiesel has attracted great attentions in recent years because of its similar properties to fossil diesel and gained widespread acceptance as its sustainability.[6] Most common method in biodiesel industry is transesterify crude oil to biodiesel with liquid potassium or sodium hydroxide[7], but the liquid catalysts are difficult to be recycled as they are soluble in methanol and glycerol mixture. So, they are usually neutralized that increases wastewater treatment cost[8]. Heterogeneous catalysts, such as hierarchically ordered nanoporous base catalyst[9], activated Zn-Al hydrotalcites[10], MgO nanocrystals[11] Li-CaO[12], CaO-La_2O_3 and CaO-CeO_2[13] are widely studied to replace homogeneous bases. Na_2SiO_3[14] and Na doped SiO_2 solid bases[15] were used for biodiesel synthesis, and the deactivated Na_2SiO_3 could be still applied for the hydrothermal production of hydrogen from by-product glycerol combined with addition of nickel catalyst[16]. However, the separation of these heterogeneous catalysts needs filtration or centrifugation that is energy and time consuming.[9-16]

Magnetic heterogeneous catalysts were easily separated from product mixture by a magnet[17] with high mass recovery rate, e.g., the rate for Na_2SiO_3/Fe_3O_4 magnetic catalyst is 1.7 times that for non-magnetic base Na_2SiO_3 (92.2 *vs.* 54.4 wt%)[18]. It was found that the recovery rate of magnetic carbon-based $Na_2SiO_3@Fe_3O_4/C$ catalyst after 5 cycles is even higher than that of Na_2SiO_3/Fe_3O_4 after 1 cycle (96.1 *vs.* 92.2 wt%) because active carbon has good loading capacity besides as reducing agent for Fe_2O_3.[19] Magnetic $Na_2SiO_3@Fe_3O_4/C$ is active for biodiesel production and easily separated, but after deactivation from biodiesel production, the remained Fe_3O_4 core is not active for

glycerol conversion to other value-added products. It is found that Ni (besides magnetic properties[20]) can catalyze glycerol to hydrogen[21], acetol and syngas[22]. For carbon supported nickel catalyst (Ni/C), NiO could be reduced by carbon carrier to active metal Ni directly without using reducing gas during pyrolysis at 700 °C for the production of porous char for catalyst loading, while commercial Ni/Al_2O_3 catalyst for H_2 production *via* steam methane reforming reaction was prepared with reducing gas (e.g., 3/7 mixture of H_2/N_2) at 750 ºC for 20 h[23].

This work is to synthesize a magnetic base catalyst (Na_2SiO_3@Ni/C) that is active for biodiesel production, easily separated for recycles, and H_2 production from glycerol after deactivation. The catalyst was tested in biodiesel production from soybean oil and further for the hydrothermal production of hydrogen from by-product (crude glycerol) in biodiesel production.

2. Experimental

2.1. Materials

Bamboo powders [49.4 C, 6.0 H and 43.4 O, wt%; analyzed by Elemental Analyzer (Vario EL III CHONS, Elementar Analysensysteme GmbH, Hanau, Germany)] were purchased from Zhili Hongqiang bamboo processing plant (Huzhou, Zhejiang), dried in an oven (WFO-710, EYELA, Tokyo Rikakikai Co., Ltd.) at 105 ^oC for 24 h, ball-milled (SHQM-0.4L, Chunlong Petroleum Instrument Co., Ltd., Lianyungang, Jiangsu) and passed through a 200-mesh sieve for experiments. Deionized water was obtained by a water purification system (electrical conductivity is 18.2 MΩ·cm, Milli-Q Academic, Merck Millipore, Darmstadt, Germany). Analytical reagents $Ni(NO_3)_2 \cdot 6H_2O$ (≥ 98.0%), urea (≥ 99.0%), sodium silicate nonahydrate ($Na_2SiO_3 \cdot 9H_2O$, 19.3-22.8 wt% Na_2O, weight ratio of Na_2O/SiO_2 = 1.03±0.03), dehydrated methanol (≥ 99.5%), glycerol (≥ 99.0%), Na_2CO_3

(99.8%) and potassium hydrogen phthalate [$C_6H_4(COOK)(COOH)$, 99.5%] were purchased from Xilong Chemical Factory Co., Ltd. (Shantou, Guangdong). Soybean oil [refined, molecular weight of 881.2 g/mol, acid value (AV) of 0.6 mg KOH/g] was bought from Jiali Cereal & Oil Co., Ltd. (Fangchenggang, Guangxi). Standard heptadecanoic acid methyl ester ($C_{17:0}$) and other methyl esters [palmitate ($C_{16:0}$), linolenate ($C_{16:1}$), stearate ($C_{18:0}$), oleate ($C_{18:1}$), linoleate ($C_{18:2}$) and linolenate ($C_{18:3}$)] (≥ 99.0%) were purchased from Sigma (Shanghai). Crude glycerol [94.7 wt% glycerol, 5.3 wt% unreacted oil, biodiesel and methanol; TOC (total organic carbon) of 32.7 mmol/g] was produced during soybean biodiesel production catalyzed by Na_2SiO_3@Ni/C during 1-4 catalyst cycles and distilled at 65 ^oC for 2 h by a rotary evaporator (RE-52AA, Shanghai Yancheng Instrument Co., Ltd.).

2.2. Catalyst preparation

Similar to previous work[19], aqueous solution (500 mL) of $Ni(NO_3)_2 \cdot 6H_2O$ (145.5 g), solid urea (60 g) and bamboo powders (24 g) were added into a three-neck flask (1 L) with a water-cooled condenser. The flask was submerged in oil bath at 135 °C with vigorous mechanical stirring for 10 h for reaction to form $Ni(OH)_2$ by ammonium hydroxide caused by slow urea decomposition in hot water [$CO(NH_2)_2 + H_2O \rightarrow NH_3\uparrow + CO_2\uparrow + NH_4OH$; $Ni(NO_3)_2 + NH_4OH \rightarrow Ni(OH)_2\downarrow + NH_4NO_3$]. After filtered (pore size 1-3 μm) and washed with deionized water, solid product was dried at 105 °C and heated 2 h to reach 700 °C for 2 h calcination in a tubular furnace (SGL-1100, Shanghai Daheng Optics and Fine Mechanics Co., Ltd.) under nitrogen flowing (200 mL/min) to form Ni particles (Ni plays both roles as magnetic carrier and catalytic site for H_2 production) by dehydration and reduction [$Ni(OH)_2 \rightarrow NiO + H_2O$; $NiO + C \rightarrow Ni + CO/CO_2\uparrow$] while the formed porous char is as

support to load Na_2SiO_3. Ni/C particles (20 g) were put into aqueous sodium silicate solution (150 mL containing 60 g $Na_2SiO_3 \cdot 9H_2O$) in a flask (1 L) and stirred at 85 °C in oil bath to achieve a gel by evaporation. The dried gel was heated 2 h to reach 400 °C for 2 h calcination in the tubular furnace under nitrogen flowing (200 mL/min), and milled by the above ball-mill with ZrO_2 balls at spinning speed of 230 rpm for 12 h, and sieved through 200-mesh. The obtained catalyst (powders) was designated as Na_2SiO_3@Ni/C (containing 56.0 wt% Na_2SiO_3). Na_2SiO_3 catalyst was prepared by calcining $Na_2SiO_3 \cdot 9H_2O$ at 400 °C for 2 h, and then passed through 100-mesh sieve after ground by a mortar.

After biodiesel reaction in a sealed glass reactor, liquid products were decanted, catalyst remained in the reactor attracted by a magnet (NeFeB, Ø37 mm×H18 mm) was directly used for next runs without any treatment. After 5 cycles, the catalyst was washed by ethanol under magnetic stirring thoroughly, dried at 105 °C until consistent weight (denoted as deactivated Na_2SiO_3@Ni/C) for hydrothermal gasification, and recovery rate was calculated as:

Recovery rate (wt %) = (weight of deactivated Na_2SiO_3@Ni/C) / (weight of fresh Na_2SiO_3@Ni/C ×100% (1)

After gasification, the deactivated Na_2SiO_3@Ni/C catalyst was separated by the magnet, washed by water, dried at 105 °C until consistent weight, and denoted as used deactivated Na_2SiO_3@Ni/C for characterization.

2.3. Catalyst characterization

Ni/C, fresh, deactivated and used deactivated Na_2SiO_3@Ni/C catalysts were analyzed by X-ray diffraction (XRD; Rigaku Rotaflex RAD-C, Tokyo) using a CuKα radiation source. Their functional

groups were detected by Fourier transform-infrared spectroscopy (FT-IR; Nicolet iS10, Thermo Fisher Scientific Co., Ltd., Waltham, MA) over the range from 400 to 4000 cm^{-1} with a resolution of 0.4-4 cm^{-1} using the standard KBr disk method. Magnetic properties of catalysts were measured by using a vibrating sample magnetometer (VSM; lakeshore7407, Lake Shore Cryotronics, Inc., Westerville, OH). Their morphologies were examined using a scanning electron microscope (SEM; Quanta 200, FEI, Hillsboro, OR). Selected surface areas in samples were analyzed by energy-dispersive X-ray spectrometry (EDX; Quanta 200, Hillsboro, OR) to obtain semi-quantitative elemental compositions (C, O, Ni, Na and Si excluding H). Inductively Coupled Plasma-Optical Emission Spectrometer (ICP-OES; Optima 5300 DV, PerkinElmer Inc., Waltham, MA) was used to analyze inorganic Ni, Na and Si compositions of catalysts after dissolved by HCl. Specific surface area and pore volume of samples were determined by Bruner Emmett and Teller (BET) method (Tristar II 3020, Micromeritics Instrument Co., Ltd., Northcross, GA). Temperature programmed desorption (TPD; Chemisorption analyzer, Quantachrome Instruments, Boynton Beach, FL) was applied to assess the basicity of catalysts. In TPD analysis, sample (about 50-100 mg) was degassed by heating to 400 °C (5 °C/min) and cooled to 50 °C exposed with He flowing (85 mL/min), and absorbed CO_2 by flushing pure CO_2 (85 mL/min) for 80 min. The sample was subsequently desorbed by heating to 400 °C (5 °C/min) and kept for 60-90 min under He flowing (85 mL/min). Four different volumes (0.5, 1, 1.5 and 2 mL) of standard CO_2 gas (10% CO_2 and 90% helium) were used to calibrate the basicity.

2.4. Biodiesel production and analysis

Biodiesel production was carried out in a 20 mL glass reactor (Ø25 mm×H55 mm). Refined

soybean oil (4.4-4.6 g), a relevant amount of dehydrated methanol and catalyst were mixed and stirred by a magnetic bar (15 mm length) in the glass that was sealed by a cover with silicon rubber washer (Fig. 1a) and immersed in oil bath at 55-75 ^{o}C for reaction. All the experiments were repeated at least two times, and the reported biodiesel yields were averaged data with standard deviation (σ) of 0.05-4.25 %.

After reaction, crude biodiesel at upper layer (Fig. 1b) was collected and filtered (pore size 0.22 μm) for analysis by Gas Chromatography (GC; GC-2014, Shimadzu, Kyoto) with a capillary column of Rtx-Wax (30 m×Ø0.25 mm×0.25 μm) under analytical conditions of column temperature 220 °C, injector temperature 260 °C, detector temperature 280 °C, carrier gas (He) with flow rate 1 mL/min and split ratio 40/1. Biodiesel yield (weight calculated by GC peaks/actual weight of crude biodiesel ×100%, wt%) was determined by using heptadecanoic acid methyl ester (HDAM; $C_{17:0}$) as internal standard. The relative response factor of six standard methyl esters [palmitate ($C_{16:0}$), linolenate ($C_{16:1}$), stearate ($C_{18:0}$), oleate ($C_{18:1}$), linoleate ($C_{18:2}$) and linolenate ($C_{18:3}$)] to that of HDAM was calibrated as 1.014, 1.023, 1.076, 1.038, 1.019 and 0.926 in previous work[17].

2.5. Hydrothermal gasification of glycerol and analysis

Similar to previous work[16], subcritical water gasification of glycerol was conducted in a Hastelloy (HC-276) autoclave (25 mL with 8.4 mL headspace, Parr Instrument Co., Moline, IL). The autoclave can reach temperature and pressure up to 500 °C and 34.5 MPa, respectively. In each experiment, water (15 g), glycerol (0.41-0.49 g) and a relevant amount of catalyst were added to the autoclave and sealed. Then, nitrogen (99.999% purity) was added and purged for 3 times to remove air, and an initial nitrogen pressure of 8.0 MPa was used to avoid water vaporization during

gasification. The autoclave was heated from room temperature (20 °C) and took 55 min to reach 350 °C and 21.5-22.0 MPa and kept for 5 min reaction time with magnetic stirring (250 rpm). The reactor was powered off and immediately cooled down to room temperature by an electric fan for 2 h. Gas volume (about 2.44-3.12 L) was measured using a wet gas meter (LMF-1, Shanghai A.K. Instruments Co., Ltd.), where water was saturated by $NaHCO_3$ to avoid absorption of CO_2. Gas was collected in a gas bag for GC analysis. The aqueous sample was collected and centrifuged for further analysis. Each experiment was repeated at least two times, and the reported data were averaged values.

Produced gas (H_2, CO_2, C_2H_6, C_2H_4 and C_2H_2) was analyzed by GC (7820A, Agilent, Palo Alto, CA) with a packed column Porapak N (3 ft × 1/8 in.) and a thermal conductivity detector (TCD). CH_4 and CO were analyzed by the same GC with a packed column Molecular Sieve 5A (6 ft × 1/8 in.) and a TCD. Helium and N_2 (99.999% purity) were used as carrier gas. Gas sample was calibrated with three different concentrations diluted with N_2 from a standard gas mixture (9.082% H_2, 6.063% CO, 6.013% CH_4, 6.029% CO_2, 0.100% C_2H_6, 0.106% C_2H_4 and 0.100% C_2H_2; vol%) (Yunnan Messer Co., Ltd., Kunming) (with R^2 of 0.9837 for H_2, 0.9906 for CO_2, 0.9967 for CH_4 and CO for 0.9970).

Mole of gas (n_i) was calculatd as:

$$n_i \text{ (mole)} = P_0 V_i / (RT) \quad (2)$$

Where n_i (mole) and V_i (m^3) are mole and volume of H_2, CO, CH_4 and CO_2; P_0 (0.8×10^5 Pa) is atmospheric pressure at altitude 1886.5 m in Kunming[24] (north latitude 25.00°, east longitude 102.39°) calculated by Barometric formula[25]; R is gas constant (8.31 mol·K/Pa·m^3) and T is gas temperature (298 K).

Gas composition was defined as:

Gas (mol%) = (mole of gas) / (total mole of H_2, CO_2, CH_4 and CO) × 100% (3)

Where gas is for H_2, CO_2, CH_4 and CO, respectively (C_2 gases < 0.01%).

Gasification rate was defined as:

Gasification rate (mol%) = (carbon mole of CO_2, CH_4, CO and inorganic carbon) / (carbon mole of crude glycerol) × 100% (4)

Inorganic carbon (IC) and TOC of aqueous products and crude glycerol were measured with a TOC analyzer (TOC-V_{CPN}, Shimadzu, Kyoto) using Na_2CO_3 and $C_6H_4(COOK)(COOH)$ as standard IC (25, 50 and 100 ppm; $R^2 \geq 0.999$) and TOC (250, 500 and 1000 ppm; $R^2 \geq 0.999$) calibrants. Crude glycerol produced was determined with a high performance liquid chromatography (HPLC; LC-20A, Shimadzu) fitted with an HPX-87H column and a reflex index (RI) detector.

3. Results and discussion

Biodiesel from soybean oil was produced in the glass reactor and its by-product glycerol was further gasified in the autoclave. Experimental setup and catalyst separation for biodiesel production with Na_2SiO_3@Ni/C catalyst are given in Fig. 1. Figs. 2 shows biodiesel yield versus variables according to single-factor experiments. Characteristic results of XRD, FT-IR, VSM, SEM, EDX, BET and CO_2-TPD for catalysts are presented in Figs. 3-8, respectively. Elemental compositions of catalysts by ICP-OES and EDX are listed in Table 1. Temperate and pressure profiles, and gas products from hydrothermal gasification of glycerol are illustrated in Figs. 9-11. Glycerol gasification rate, gas concentrations and carbon balance in hydrothermal gasification of glycerol are summarized in Tables 2 and 3. Deactivated catalyst after gasification is characterized with results

given in Fig. 12.

3.1. Biodiesel production

Effects of variables [i.e., methanol/oil molar ratio (3/1-15/1), catalyst dosage (3-11 wt%) reaction temperature (55-75 °C), and reaction time (40-120 min)] on biodiesel yield from soybean oil were optimized according to single-factor experiments in the glass reactor (Fig. 1).

3.1.1. Methanol/oil molar ratio

In Fig. 2a, biodiesel yield was just 55.1% when theoretical methanol/oil molar ratio of 3/1 was used at 65 °C for 100 min with 7 wt% catalyst owing to the heterogeneous reaction conditions and insufficient methanol for transesterification caused by methanol evaporation and mixture.[19] As methanol/oil molar ratio rose from 6/1 to 9/1, biodiesel yield reached the highest of 97.9% from 90.2%, and dropped gradually to 93.9% and 87.9% at methanol/oil ratio of 12/1 and 15/1. This might be due to the relative low concentration of catalyst in the reaction system caused by excess methanol. Methanol/oil molar ratio of 9/1 is selected as the best value for the next experiments.

3.1.2. Catalyst dosage

In Fig. 2b, catalyst increased from 1 to 9 wt% for biodiesel production under conditions of methanol/oil molar ratio of 9/1, reaction temperature of 65 °C and reaction time of 100 min. Biodiesel yield jumped sharply from 84.2% to 91.0% as catalyst rose from 1 to 3 wt%, and grew slightly to 94.9% at 5 wt% before reached the highest value of 97.9% at 7 wt% catalyst. Low amount of solid catalyst 1 wt% was insufficient for transesterification, and > 5 wt% catalyst was required for

reaction. However, as catalyst increased further from 7% to 9 wt%, biodiesel yield declined slightly because of the difficult mixing of liquid reactants with high concentration of catalyst under magnetic stirring. Catalyst of 7 wt% with the highest yield of 97.9% is selected as the best value for the next optimization.

3.1.3. Reaction temperature

Temperature from 55 to 75 °C was optimized for biodiesel production under conditions of reaction time of 100 min, methanol/oil molar ratio of 9/1 and catalyst of 7 wt% (Fig. 2c). Biodiesel yield reached 92.6% at 55 °C due to long reaction time (100 min) for transesterification at low temperature. The yield increased slowly from 95.9% to the highest value of 97.9% as temperature grew from 60 to 65 °C, and gradually decreased to 96.3% and 94.3% at 70 and 75 °C. This is because that high temperature promoted reaction to reach higher biodiesel yield, but liquid methanol vaporized into gas phase at much higher temperature, and resulted in lower yield[26, 27]. Therefore, in this work, the best temperature is chosen as 65 °C.

3.1.4. Reaction time

Effect of reaction time on transesterification was studied from 40 to 120 min under conditions of methanol/oil molar ratio of 9/1, catalyst of 7 wt% and reaction temperature of 65 °C (Fig. 2d). As time rose from 40 to 60 min, biodiesel yield increased from 85.7% to 93.7% sharply, and gradually grew to 96.5% at 80 min and the highest value of 97.9% at 100 min. There is no obvious rise (98.5% *vs.* 97.9%) when time rose further to 120 min. The best reaction time is chosen as 100 min.

Therefore, the best conditions are 9/1 methanol/oil molar ratio and 7 wt% catalyst at 65 °C for

100 min with biodiesel yield of 97.9%.

3.1.5. Catalyst cycles

Recycle studies of Na_2SiO_3@Ni/C catalyst were carried out under the best conditions (i.e., 65 °C for 100 min, 9/1 methanol/oil molar ratio and 7 wt% catalyst) optimized by the above single-factor experiments. Magnetically separated catalyst was directly used for next runs without any treatment. Biodiesel yield decreased little for the first 3 cycles (97.9±0.60%, 98.1±0.345 % and 97.0±0.265 %), but the yield dropped to 93.1±0.575 % and 80.9±1.91 % at the fourth and fifth cycle. After 5 cycles, recovery rate of Na_2SiO_3@Ni/C was 85.6±2.97 wt%. The deactivation of catalyst might be caused by the leaching of active component (Na_2SiO_3) in methanol[19] that also catalyzed transesterification. Previous work[14] showed that calcined sodium silicate (Na_2SiO_3) after washed for 5 times with methanol still had high activity with biodiesel yield > 90% from soybean oil at 60 ºC for 120 min, but the corresponding recovered methanol with leached active component had a lower biodiesel yield (< 65%). It also confirmed that the main transesterification reaction started on the surface of Na_2SiO_3.

In this work, magnetic stirring was applied in biodiesel experiments. Although there were numerous Na_2SiO_3@Ni/C particles attached on the magnetic bar's surface before and after reaction (Fig. 1), but the particles were dispersed well during stirring at about 750 rpm by centrifugal force to promote biodiesel production. For industry application, mechanical stirring can be used with electromagnet recovered system. On the other hands, electromagnetic reactor could be designed to have better mixing for reactants and catalyst. Characterization of catalysts before and after reaction was studied further in the next section.

3.2. Catalyst characterization

3.2.1. XRD

The crystalline phases of Ni and Na_2SiO_3 in the Ni/C particles and catalysts were determined by XRD analysis (Fig. 3) as compared with the cards from Joint Committee on Powder Diffraction Standards (JCPDS: 04-0850, 16-0818). Ni/C particles have well-crystallized Ni structures with characteristic and symmetric reflections, but there is no peak from the active carbon because of its undefined structure (Fig. 3a). Fresh Na_2SiO_3@Ni/C has well-crystallized structures of Na_2SiO_3 and Ni (Fig. 3b). But, the characteristic reflections from Na_2SiO_3 almost disappeared after 5 cycles (Fig. 3c), proving its leaching into methanol.

3.2.2. FT-IR

In Fig. 4, absorptions at 3424 and 1637 cm^{-1} are observed for all samples due to the stretching and bending vibrations of –OH groups[28] from physically adsorbed water, and their intensity could be reduced by heat treatment.[29] Ni/C particles have no other obvious absorption except those for –OH (Fig. 4a). This means that carbon support in Ni/C particles (12.7%, Table 1) was almost carbonized completely, and NiO was reduced by carbon completely because of no absorption found at 430 cm^{-1} for Ni-O.[30] After loading Na_2SiO_3, Na_2SiO_3@Ni/C catalyst has many obvious absorptions at 1025, 960, 889 and 710 cm^{-1} from Si-O bending, Si-O-Na, Si-O-H and Si-O-Si stretching, respectively.[14] The bands from 745 to 467 cm^{-1} are contributed from symmetric stretching and bending vibrations of Si-O-Si bond[31]. Furthermore, an absorption at 1462 cm^{-1} from CO_3^{2-} groups was possibly from the reaction of CO_2 in air with Na_2SiO_3 during sample

preparation.[29] However, absorptions for deactivated Na_2SiO_3@Ni/C catalyst became weak (Fig. 4c), because Na_2SiO_3 was leached after 5 cycles, which was also confirmed by XRD analysis (Fig. 3a).

3.2.3. VSM

Hysteresis loops measurement gives specific magnetic saturation values (Ms). Ms of fresh Na_2SiO_3@Ni/C (15.7 Am^2/kg) is lower than that of Ni/C particles (41.8 Am^2/kg) after covered with 130 wt% Na_2SiO_3 (Fig. 5a and b) but with much stronger magnetism than that of Na_2SiO_3/Fe_3O_4 catalyst prepared in previous work (15.7 *vs.* 0.5 Am^2/kg)[18]. So, the prepared catalyst is easily separated by a magnet for recycles (Fig. 1b). After 5 cycles, its Ms slightly decreased to 15.3 Am^2/kg (Fig. 5c *vs.* b). The magnetism of Na_2SiO_3@Ni/C catalyst is strong and stable.

3.2.4. SEM, EDX and ICP-OES

In Fig. 6A-a, Ni/C particles have bulk structure of fibrous shape (< 100 μm) similar to that of original bamboo. At larger magnification, numerous spherical Ni particles (0.3-1 μm) are found, demonstrating they were well-precipitated on the surface of carbon support. EDX spectrum (Fig. 6A-b) shows that they were mainly composed of (wt%) 96.4 Ni and 2.60 C with minor of O (0.70) and trace of Na (0.10) and Si (0.20) (Na and Si were apparently from inorganics in bamboo as ash). EDX data were semi-quantitative for the selected surface areas.[32, 33] ICP is for the whole bulk sample analysis, and it revealed much lower Ni content (87.3 wt%) for Ni/C particles (Table 1) because $Ni(OH)_2$ was precipitated and concentrated on the surface of bamboo powders. Ni/C particles contained 12.7 wt% (100% - Ni%) bamboo char for subsequent loading base Na_2SiO_3.

Na_2SiO_3@Ni/C catalyst doesn't have uniformed particle size in bulk (< 50 μm) with small

particles agglomerated by Na_2SiO_3 gel (Fig. 6B-a). It was composed of (wt%) C (5.00), O (18.1), Na (30.7), Si (14.3) and Ni (31.9) analyzed by EDX in a selected area (Fig. 6B-b). Na/Si molar ratio of Na_2SiO_3@Ni/C by EDX is 2.0/0.8 (higher than 2/1 for Na_2SiO_3 and for ICP analysis in Table 1). This is because Na_2SiO_3 solution was hydrolyzed to NaOH and H_2SiO_3 [$Na_2SiO_3 + H_2O \rightarrow NaOH + H_2SiO_3$], more of H_2SiO_3 or SiO_2 remained on the core of Na_2SiO_3@Ni/C catalyst after dry and calcination.

After 5 cycles, the morphology of Na_2SiO_3@Ni/C catalyst changed little (Fig. 6C-a), but its C increased to 28.5 wt% from 5.00 wt% by EDX analysis because residual glycerol, biodiesel and oil deposited on the surface of catalyst. ICP analysis shows that its Ni also rose to 75.6 wt% from 38.4 wt%, and Na and Si decreased to 8.21 and 5.09 wt% from 20.6 and 12.5 wt% (Table 1) because Na_2SiO_3 was leached, that was also confirmed by XRD pattern in Fig. 3c.

3.2.5. BET

Nitrogen adsorption-desorption isotherm (Fig. 7a) shows that Ni/C particles exhibited a clear hysteresis loop with high adsorption capacity (76.1 m^2/g specific surface area and 0.101 cm^3/g pore volume). The high specific surface area was caused by pyrolysis of bamboo and reduction of NiO with carbon at 700 °C to form numerous micropores in biochar by vaporization of volatiles and gases. After loading Na_2SiO_3, the specific surface area and pore volume of Na_2SiO_3@Ni/C were significantly declined to 8.24 m^2/g and 0.047 cm^3/g because pores were filled by Na_2SiO_3 as compared with specific surface area of 2.42 m^2/g for calcined Na_2SiO_3. After 5 cycles, they increased to 14.3 m^2/g and 0.052 cm^3/g because Na_2SiO_3 was leached.

3.2.6. CO_2-TPD

In Fig. 8, Ni/C particles have no obvious CO_2 desorption with a very weak basicity of 0.01 mmol/g. Na_2SiO_3@Ni/C catalyst has two peaks at 260-300 ℃ and 360-400 ℃ for CO_2 desorption with total basicity of 3.18 mmol/g. But, the basicity reduced significantly to 0.29 mmol/g after 5 cycles because some Na_2SiO_3 was leached and the active sites were covered by glycerol, oil and soap.

3.3. Hydrothermal gasification

After 5 cycles, deactivated Na_2SiO_3@Ni/C was ethanol-washed and selected as catalyst for H_2 production in the autoclave from biodiesel byproduct glycerol (both pure and crude glycerol were used as feedstocks in the experiments) at 350 ℃ under 21.5-22.0 MPa for 5 min (heating time from 20 to 350 ℃ need 55 min under 8.0 MPa initial N_2 pressure. Fig. 9 shows that reaction temperature and pressure rapidly rises to 340 ℃ and 21.8 MPa at 31 min from 25 ^{o}C and 8 MPa, and gradually increases further to 350 ^{o}C and 22.0 MPa at 55 min for 5 min in a typical run.

3.3.1. Gasification of pure glycerol

In Fig 10a, a blank experiment was conducted to gasify pure glycerol (total carbon of 15 mmol) without catalyst, and results showed very low gas yield produced (0.102 mmol H_2, 0.00352 mmol CO, 0.0702 mmol CH_4, and 0.468 mmol CO_2). However, when 10 wt% deactivated Na_2SiO_3@Ni/C catalyst was added, H_2, CO, CH_4 and CO_2 sharply jumped to 5.59, 0.989, 1.60 and 4.08 mmol, respectively. As catalyst rose to 20 and 30 wt%, H_2 production increased further to 7.17 and 11.7 mmol, CO_2 to 5.43 and 6.62 mmol, but slight rise for CH_4 (2.13 and 2.28 mmol). These results indicated that hydrothermal gasification was efficiently promoted by Na_2SiO_3@Ni/C catalyst that

had a good activity for C-C scission followed by water-gas shift reaction ($C_3H_8O_3 + H_2O \rightarrow CO_2 + H_2$).[25, 34] As catalyst rose to 40 and 50 wt%, H_2 grew slightly to 12.1 and 12.4 mmol, CO_2 to 6.80 and 7.72 mmol, but CH_4 increased obviously to 6.80 to 7.72 mmol, and CO reached a peak of 0.989 mmol and decreased to 0.0364 mmol because of methanation reaction ($CO + H_2 \rightarrow CH_4 + H_2O$[35]). So, 30 wt% deactivated Na_2SiO_3@Ni/C catalyst was fixed for hydrothermal gasification to study the effect of addition of calcined Na_2SiO_3.

Low H_2 concentration (56.2 mol%) was obtained with relative high concentrations of CO_2 (31.8 mol%) and CH_4 (10.9 mol%) with 30 wt% deactivated Na_2SiO_3@Ni/C (Table 2), calcined Na_2SiO_3 (20, 40, 60, 80 and 100 wt%) was added for glycerol hydrothermal gasification to promote H_2 production (Fig. 10b). H_2 production only increased slightly from 11.7 to 12.1 and 12.9 mmol, but CO_2 decreased from 6.62 to 6.31 and 1.60 mmol as Na_2SiO_3 rose from 0 to 20 and 100 wt%. Na_2SiO_3 had little promotion for H_2 production but could absorb CO_2 by dissolving it into the basic hydrothermal solution to form Na_2CO_3 ($CO_2 + H_2O + Na_2SiO_3 \rightarrow Na_2CO_3 + H_2SiO_3$). The CO_2 absorption was also confirmed by IC in aqueous-phase increasing from 9.50 to 63.5 mol% as Na_2SiO_3 rising from 0 to 100 wt%. At the same time, carbon in gas-phase decreased from 60.8 to 17.1 mol% with low CO_2 concentration (11.8 mol%) and high H_2 concentration (83.4 mol%) (Table 2). Glycerol gasification rate also rose to 80.6 mol% from 70.3 mol% without adding Na_2SiO_3. This is because Na_2CO_3 could inhibit glycerol carbonizing[36] and promote glycerol gasification similar to the case of hydrothermal gasification and liquefaction of biomass.[37] Total carbon in gas and aqueous-phases is higher (99.0 *vs.* 93.5 mol%) but organic carbon in aqueous-phase is lower (18.4 *vs.* 23.2 mol%) with addition of 100 wt% Na_2SiO_3 as compared without Na_2SiO_3, suggesting Na_2SiO_3 promoted gasification and inhibited char formation (Table 3).

3.3.2. Gasification of crude glycerol

Crude glycerol (total carbon 15.0 mmol) from the above biodiesel production was hydrothermally gasified with deactivated Na_2SiO_3@Ni/C (30 wt%) and Na_2SiO_3 (100 wt%), hydrogen rich gas (12.8 H_2, 0.0214 CO, 0.859 CH_4 and 1.80 CO_2, mmol) was produced (Fig. 11). There were no significant changes in gasification rate and gas composition between crude glycerol (80.1% with 82.7 H_2, 0.14 CO, 5.56 CH_4 and 11.6 CO_2, mol%) and pure glycerol (80.6% with 83.4 H_2, 0.11 CO, 4.72 CH_4 and 11.8 CO_2, mol%) (Tables 1 and 2). This proves that by-product crude glycerol is suitable for hydrothermal hydrogen production.

3.4. Stabilization of Ni/C after gasification

After gasification, XRD pattern shows that the used deactivated Na_2SiO_3@Ni/C after dried at 65 ºC still had well-crystallized structures of Ni but without characteristic peaks of Na_2SiO_3 because the crystal structure of Ni is stable and Na_2SiO_3 dissolved in water after hydrothermal gasification (Fig. 12a). IR spectrum also proves the disappearance of absorptions from Na_2SiO_3 (Fig. 12b). After gasification, its Ms increased to 28.7 Am^2/kg (Fig. 12c) from 15.3 (Fig. 5c), lower than that for Ni/C (41.8 Am^2/kg). Its specific surface area and pore volume also rose from 14.3 m^2/g and 0.052 cm^3/g (Fig. 7c) to 63.7 m^2/g and 0.086 cm^3/g (Fig. 12d), slightly lower than the values for Ni/C particles (76.1 m^2/g and 0.101 cm^3/g). These results confirmed that the Ni/C structure is relative stable after biodiesel production and gasification.

The deactivated Na_2SiO_3@Ni/C after gasification was recycled for hydrothermal gasification of glycerol at the same condition [Experimental conditions: 0.46 g (total carbon 15 mmol) pure glycerol, 15 g H_2O, 30 wt% used deactivated Na_2SiO_3@Ni/C, 100 wt% Na_2SiO_3, 55 min heating

time from 20 to 350 ºC and 5 min holding time, 8.0 MPa initial pressure, 22.0 MPa highest reaction pressure]. Slight higher H_2 (13.6±0.219 *vs.* 12.9±0.178 mmol) and CO_2 (1.79±0.169 *vs.* 1.60±0.257 mmol), and little change in CO (0.017±0.00436 *vs.* 0.018±0.00169 mmol) and CH_4 (0.665±0.129 *vs.* 0.661±0.106 mmol) were found as compared with that for the first used deactivated Na_2SiO_3@Ni/C. This indicates that the catalyst is still active for H_2 production.

4. Conclusions

Magnetic Na_2SiO_3@Ni/C catalyst was successfully synthesized for biodiesel and H_2 co-production from soybean oil. The catalyst was active to produce biodiesel with maximum yield of 98.1% at 65 ^oC and was easily separated by a magnet for 4 cycles (biodiesel yield > 93%). After 5 cycles, the deactivated catalyst successfully catalyzed gasification of biodiesel by-product (crude glycerol) with 80.6 mol% gasification rate and 83.4 mol% H_2 concentration in compressed water at 350 ^oC. After gasification, it is found that the structure of Ni/C changed slightly and can be re-loaded Na_2SiO_3 for both biodiesel and H_2 production from soybean oil without pollutants produced.

Acknowledgements

The authors wish to acknowledge the financial support from Nanjing Agricultural University, Chinese Academy of Sciences [CAS 135 program (XTBG-T02), Equipment R&D grant (No.YZ201260) and Open project of key laboratory of tropical plant resources and sustainable use (No. TPR201404)], the Yunnan Provincial Government (Baiming Haiwai Gaocengci Rencai Jihua), and the Natural Science Foundation of China (No. 31400518).

References

1 M. Z. Jacobson, Review of solutions to global warming, air pollution, and energy security. *Energy Environ. Sci.*, 2009, **2**, 148-173.

2 Y. Zhang, L. Jin, K. Sterling, Z. Luo, T. Jiang, R. Miao, C. Guild and S. L. Suib, Potassium modified layered $Ln_{(2)}O_{(2)}CO_{(3)}$ (Ln: La, Nd, Sm, Eu) materials: efficient and stable heterogeneous catalysts for biofuel production. *Green Chem.*, 2015, **17**, 3600-3608.

3 M. Guo, J. Littlewood, J. Joyce and R. Murphy, The environmental profile of bioethanol produced from current and potential future poplar feedstocks in the EU. *Green Chem.*, 2014, **16**, 4680-4695.

4 D. Kralisch, C. Staffel, D. Ott, S. Bensaid, G. Saracco, P. Bellantoni and P. Loeb, Process design accompanying life cycle management and risk analysis as a decision support tool for sustainable biodiesel production. *Green Chem.*, 2013, **15**, 463-477.

5 S. E. Evans, J. Z. Staniforth, R. J. Darton and R. M. Ormerod, A nickel doped perovskite catalyst for reforming methane rich biogas with minimal carbon deposition. *Green Chem.*, 2014, **16**, 4587-4594.

6 E. Lois, Definition of biodiesel. *Fuel*, 2007, **86**, 1212-1213.

7 Q. Kwok, B. Acheson, R. Turcotte, A. Janès, G. Marlair, Thermal hazards related to the use of potassium and sodium methoxides in the biodiesel industry. *J. Therm. Anal. Calorim.*, 2013, **111**, 507-515.

8 A. Singhabhandhu, T. Tezuka, A perspective on incorporation of glycerin purification process in biodiesel plants using waste cooking oil as feedstock, *Energy*, 2010, **35**, 2493-2504.

9 J. J. Creasey, C. M. A. Parlett, J. C. Manayil, M. A. Isaacs, K. Wilson and A. F. Lee, Facile route to conformal hydrotalcite coatings over complex architectures: a hierarchically ordered nanoporous base catalyst for FAME production. *Green Chem.*, 2015, **17**, 2398-2405.

10 Q. Liu, B. Wang, C. Wang, Z. Tian, W. Qu, H. Ma and R. Xu, Basicities and transesterification activities of Zn-Al hydrotalcites-derived solid bases. *Green Chem.*, 2014, **16**, 2604-2613.

11 J. M. Montero, P. Gai, K. Wilson and A. F. Lee, Structure-sensitive biodiesel synthesis over MgO nanocrystals. *Green Chem.*, 2009, **11**, 265-268.

12 R. S. Watkins, A. F. Lee and K. Wilson, Li-CaO catalysed tri-glyceride transesterification for biodiesel applications. *Green Chem.*, 2004, **6**, 335-340.

13 M. Kim, C. DiMaggio, S. Yan, S. O. Salley and K. Y. Simon Ng, The effect of support material on the transesterification activity of $CaO\text{-}La_2O_3$ and $CaO\text{-}CeO_2$ supported catalysts, *Green Chem.*, 2011,

13, 334-339.

14 F. Guo, N. N. Wei, Z. L. Xiu and Z. Fang, Transesterification mechanism of soybean oil to biodiesel catalyzed by calcined sodium silicate. *Fuel*, 2012, **93**, 468-472.

15 E. Akbar, N. Binitha, Z. Yaakob, S. K. Kamarudin and J. Salimon, Preparation of Na doped SiO_2 solid catalysts by the sol-gel method for the production of biodiesel from jatropha oil. *Green Chem.*, 2009, **11**, 1862-1866.

16 Y. D. Long, Z. Fang, T. C. Su and Q. Yang, Co-production of biodiesel and hydrogen from rapeseed and *Jatropha* oils with sodium silicate and Ni catalysts. *Appl. Energy*, 2014, **113**, 1819-1825.

17 B. J. Xue, J. Luo, F. Zhang and Z. Fang, Biodiesel production from soybean and *Jatropha* oils by magnetic $CaFe_2O_4$-$Ca_2Fe_2O_5$-based catalyst. *Energy*, 2014, **68**, 584-591.

18 P. M. Guo, F. H. Huang, M. M. Zheng, W. L. Li and Q. D. Huang, Magnetic solid base catalysts for the production of biodiesel. *J. Am. Oil Chem. Soc.*, 2012, **89**, 925-933.

19 F. Zhang, Z. Fang and Y. T. Wang, Biodiesel production directly from oils with high acid value by magnetic Na_2SiO_3@Fe_3O_4/C catalyst and ultrasound. *Fuel*, 2015, **150**, 370-377.

20 N. E.Rajeevan, V. Kumar, R. Kumar, R. Kumar and S. D. Kaushik. Neutron diffraction studies of magnetic ordering in Ni-doped $LaCoO_3$. *J. Magn. Magn. Mater.*, 2015, **393**, 394-398.

21 Y. L. Zhang, Z. Shen, X. F. Zhou, M. Zhang and F. M. Jin, Solvent isotope effect and mechanism for the production of hydrogen and lactic acid from glycerol under hydrothermal alkaline conditions. *Green Chem.*, 2012, **14**, 3285-3288.

22 D. Hernandez, D. López and J. J. Fernández. Catalytic performance of Ni/La_2O_3 materials in glycerol valorization for acetol and syngas production. *Appl. Catal. A*, 2015, **499**, 13-18.

23 T. Numaguchi, K. Shoji, S. Yoshida, Hydrogen effect on α-$A1_2O_3$ supported Ni catalyst for steam methane reforming reaction. *Appl. Catal. A*, 1995, **133**, 241-262.

24 X. Qian, Y. Q. Yao, J. R. Li, J. Yin, Y. J. Zhang, L. Y. Liu, H. S. Wang, Y. H. Zhou, L. Li, X. L. You and J. L. Ma, Distribution of atmospheric water vapor content over china. *Chinese Astron. Astr.*, 2013, **37**, 212-229.

25 N. Sissenwine, M. Dubin and S. Teweles. U.S. Standard Atmosphere. U.S. Government Printing Office, Washington, D.C., 1976.

26 F. Zhang, Z. Fang and Y. T. Wang, Biodiesel production direct from high acid value oil with a

novel magnetic carbonaceous acid. *Appl. Energy*, 2015, **155**, 637-647.

27 X. Deng, Z. Fang, Y. H. Liu and C. L. Yu, Production of biodiesel from *Jatropha* oil catalyzed by nanosized solid basic catalyst. *Energy*, 2011, **36**, 777-784.

28 A. P. Rao, A. V. Rao and G. M. Pajonk. Hydrophobic and physical properties of the ambient pressure dried silica aerogels with sodium silicate precursor using various surface modification agents. *Appl. Surf. Sci.*, 2007, **253**, 6032-6040.

29 S. S. Kouassi, M. T. Tognonvi, J. Soro and S. Rossignol. Consolidation mechanism of materials obtained from sodium silicate solution and silica-based aggregates. *J. Non-Cryst. Solids*, 2011, **357**, 3013-3021.

30 D. Varshney and S. Dwivedi. Synthesis, structural, Raman spectroscopic and paramagnetic properties of Sn doped NiO nanoparticles. *Superlattices Microstruct.*, 2015, **86**, 430-437.

31 Y. Chen, G. Yu, F. Li and J. Wei. Structure and photoluminescence of amorphous silicate composites containing ZnO particles synthesized from layered sodium silicate. *J. Non-Cryst. Solids*, 2012, **358**, 1772-1777.

32 M. C. Zuluaga, A. Alonso-Olazabal, X. Murelaga and L. A. Ortega. A comparison of scanning electron microscopy energy dispersive X-ray (SEM/EDX) and inductively coupled plasma optical emission spectrometry (ICP-OES) for provenance inferences of grog-tempered Bronze Age pottery. *Microchem J.*, 2011, **99**, 443-448.

33 L. Wang, T. Li, B. M. Güell, T. Løvås and J. Sandquist. An SEM-EDX study of forest residue chars produced at high temperatures and high heating rate. *Energy Procedia,* 2015, **75**, 226-231.

34 Z. Fang, T. Minowa, C. Fang, R. L. Smith Jr., H. Inomata and J. A. Kozinski, Catalytic hydrothermal gasification of cellulose and glucose. *Int. J. Hydrogen Energy*, 2008, **33**, 981-990.

35 N. Shimoda, D. Shoji, K. Tani, M. Fujiwara, K. Urasaki, R. Kikuchi and S. Satokawa, Role of trace chlorine in Ni/TiO_2 catalyst for CO selective methanation in reformate gas. *Appl. Catal. B*, 2015, **174-175**, 486-495.

36 Z. Fang and C. Fang, Complete dissolution and hydrolysis of wood in hot water. *AIChE J.*, 2008, **54**, 2751-2758.

37 Z. Fang, T. Minowa, R. L. Smith Jr., T. Ogi and J. A. Kozinski, Liquefaction and gasification of cellulose with Na_2CO_3 and Ni in subcritical water at 350 ºC. *Ind. Eng. Chem. Res.*, 2004, **43**, 2454-2463.

Figure Captions:

Fig. 1 Biodiesel production and catalyst separation in a glass reactor: (a) before and (b) after transesterification.

Fig. 2 Effects of variables on the soybean biodiesel production with Na_2SiO_3@Ni/C catalyst: (a) methanol/oil molar ratio, (b) catalyst dosage, (c) reaction temperature, and (d) reaction time.

Fig. 3 XRD patterns of (a) Ni/C particles, (b) fresh and (c) deactivated Na_2SiO_3@Ni/C catalysts.

Fig. 4 FT-IR spectra of (a) Ni/C particles, (b) fresh and (c) deactivated Na_2SiO_3@Ni/C catalysts.

Fig. 5 Hysteresis loops of (a) Ni/C particles, (b) fresh and (c) deactivated Na_2SiO_3@Ni/C catalysts.

Fig. 6 (a) SEM images and (b) EDX spectra of (A) Ni/C particles, (B) fresh and (C) deactivated Na_2SiO_3@Ni/C catalysts (H is undetectable by EDX, and excluded in elemental composition).

Fig. 7 Nitrogen adsorption/desorption isotherms of (a) Ni/C particles, (b) fresh and (c) deactivated Na_2SiO_3@Ni/C catalysts.

Fig. 8 CO_2-TPD profiles of (a) Ni/C particles, (b) fresh and (c) deactivated Na_2SiO_3@Ni/C catalysts.

Fig. 9 Temperature and pressure versus time (0-60 min) in hydrothermal gasification of crude glycerol with deactivated Na_2SiO_3@Ni/C catalyst
[Experimental conditions: 0.46 g (total carbon 15 mmol) crude glycerol, 15 g H_2O, 55 min heating time from 20 to 350 ºC and 5 min holding time, 8.0 MPa initial pressure, 22.0 MPa highest reaction pressure.]

Fig. 10 Gas products from hydrothermal gasification of pure glycerol with various dosage of (a) deactivated Na_2SiO_3@Ni/C catalyst, and (b) Na_2SiO_3 with 30 wt% deactivated Na_2SiO_3@Ni/C catalyst.
[Experimental conditions: 0.46 g (total carbon 15 mmol) glycerol, 15 g H_2O, 55 min heating time from 20 to 350 ºC and 5 min holding time, 8.0 MPa initial pressure, 21.5-22.0 MPa highest reaction pressure.]

Fig. 11 Gas products from hydrothermal gasification of glycerol with 30 wt% deactivated Na_2SiO_3@Ni/C and 100 wt% Na_2SiO_3.
[Experimental conditions: 0.46 g (total carbon 15 mmol) glycerol, 15 g H_2O, 55 min heating time from 20 to 350 ºC and 5 min holding time, 8.0 MPa initial pressure, 22.0 MPa highest reaction pressure.]

Fig. 12 Characterization of used deactivated Na_2SiO_3@Ni/C after gasification: (a) XRD, (b) FT-IR, (c) VSM, and (d) nitrogen adsorption/desorption isotherms.

Table Captions:

Table 1 Elemental compositions (C, O, Na, Si and Ni) of Ni/C, fresh and deactivated Na_2SiO_3@Ni/C catalysts.

Table 2 Gas products from hydrothermal gasification of glycerol with deactivated Na_2SiO_3@Ni/C and Na_2SiO_3 catalysts.

Table 3 Carbon balance and glycerol gasification rate in hydrothermal gasification of glycerol with deactivated Na_2SiO_3@Ni/C and Na_2SiO_3 catalysts.

Table 1 Elemental compositions (C, O, Na, Si and Ni) of Ni/C, fresh and deactivated Na_2SiO_3@Ni/C catalysts.

Wt%	Ni/C	Fresh Na_2SiO_3@Ni/C	Deactivated Na_2SiO_3@Ni/C
C[a]	2.60	5.00	28.5
O[a]	0.70	18.1	20.9
Na[a]	0.10	30.7	18.7
Si[a]	0.20	14.3	11.7
Ni[a]	96.4	31.9	20.2
Na/Si mole ratio[a]	-	2.0/0.8	2.0/1.0
Na[b]	0.06	20.6	8.21
Si[b]	0.15	12.5	5.09
Ni[b]	87.3	38.4	75.6
Char	12.7	-	-
Na/Si mole ratio[b]	-	2.0/1.0	2.0/1.0

[a] analyzed by EDX, H is undetectable.

[b] analyzed by ICP-OES, for Ni/C, char (%) was calculated by (100% - Ni%) (Na and Si were from char as inorganic ash).

Table 2 Gas products from hydrothermal gasification of glycerol with deactivated Na_2SiO_3@Ni/C and Na_2SiO_3 catalysts.

Gas-phase composition (mol%)	Deactivated Na_2SiO_3@Ni/C[a]	Deactivated Na_2SiO_3@Ni/C and Na_2SiO_3[a]	Deactivated Na_2SiO_3@Ni/C and Na_2SiO_3[b]
H_2	56.2±2.50	83.4±1.17	82.7±2.11
CO	1.10±0.85	0.11±0.01	0.14±0.02
CH_4	10.9±0.05	4.72±0.70	5.56±0.52
CO_2	31.8±2.97	11.8±1.69	11.6±0.88
C_2(C_2H_2, C_2H_4, C_2H_6)	< 0.01	< 0.01	< 0.01

Experimental conditions: 0.46 g glycerol (total carbon 15 mmol), 30 wt% deactivated Na_2SiO_3@Ni/C after 5 cycles, 100 wt% Na_2SiO_3, 15 g H_2O, 55 min heating time from 20 to 350 ºC and 5 min holding time, 8.0 MPa initial pressure, and 22.0 MPa highest pressure.

[a] with pure glycerol.

[b] with crude glycerol.

Table 3 Carbon balance and glycerol gasification rate in hydrothermal gasification of glycerol with deactivated Na_2SiO_3@Ni/C and Na_2SiO_3 catalysts.

	Deactivated Na_2SiO_3@Ni/C[a]	Deactivated Na_2SiO_3@Ni/C and Na_2SiO_3[a]	Deactivated Na_2SiO_3@Ni/C and Na_2SiO_3[b]
Carbon in aqueous-phase (mol%)	32.7	81.9	80.8
Inorganic carbon	9.50±0.57	63.5±2.50	62.3±2.05
Organic carbon	23.2±1.03	18.4±0.95	18.5±0.87
Carbon in gas-phase (mol%)	60.8	17.1	17.8
Total (mol%)	93.5	99.0	98.6
Glycerol gasification rate (mol %)	70.3	80.6	80.1

Experimental conditions: 0.46 g glycerol (total carbon 15 mmol), 30 wt% deactivated Na_2SiO_3@Ni/C after 5 cycles, 100 wt% Na_2SiO_3, 15 g H_2O, 55 min heating time from 20 to 350 ºC and 5 min holding time, 8.0 MPa initial pressure, and 22.0 MPa highest pressure.

[a] with pure glycerol.

[b] with crude glycerol.

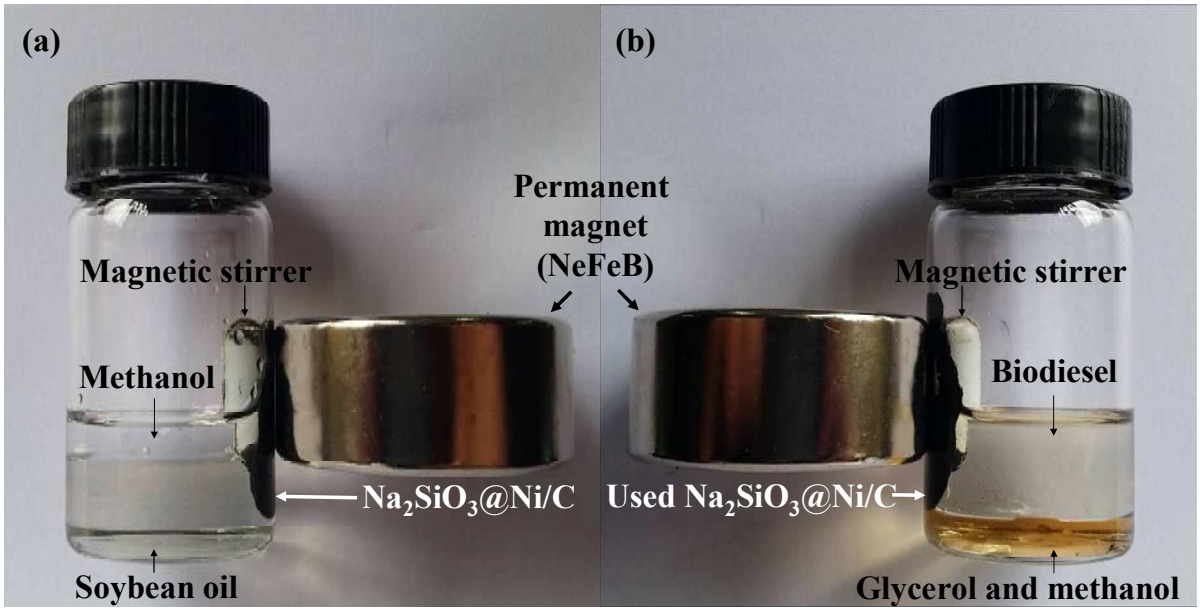

Fig. 1 Biodiesel production and catalyst separation in a glass reactor: (a) before and (b) after transesterification.

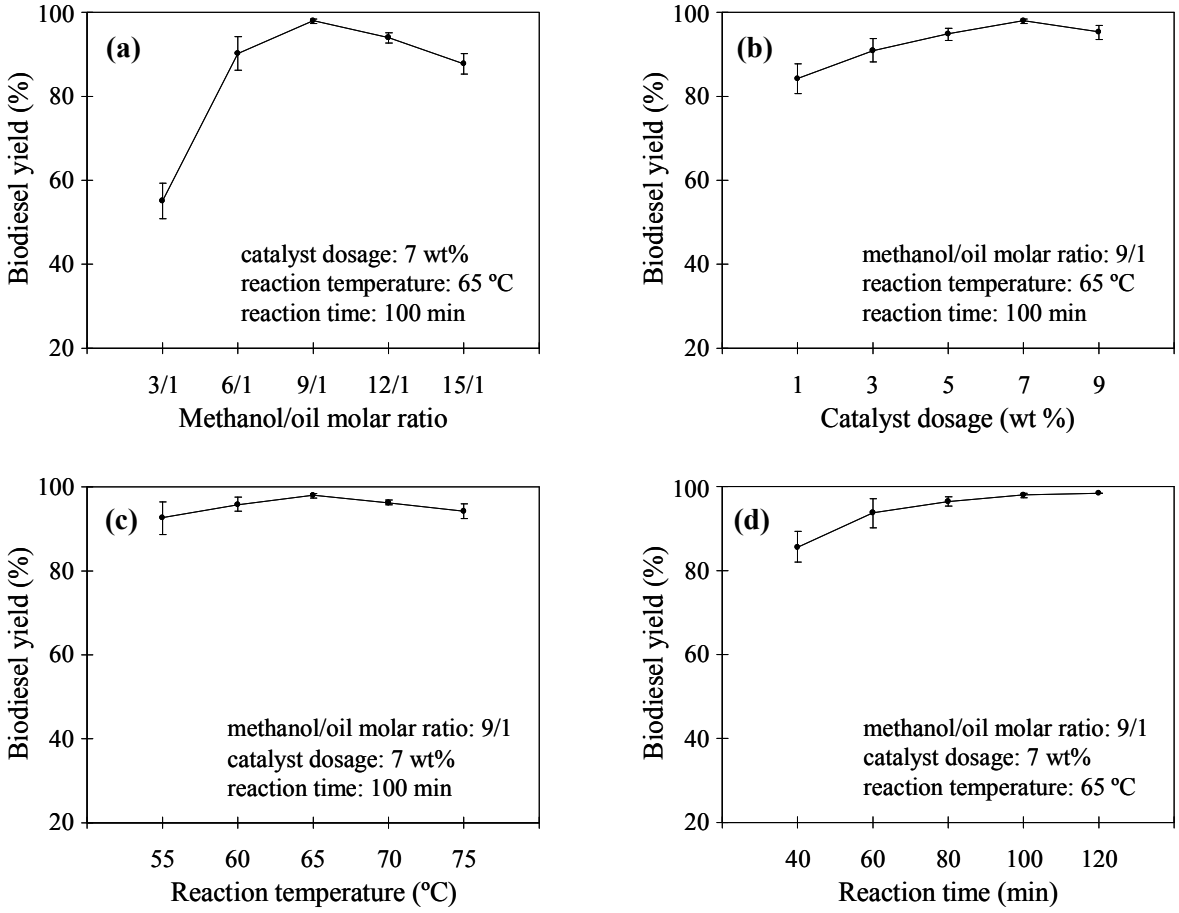

Fig. 2 Effects of variables on the soybean biodiesel production with Na_2SiO_3@Ni/C catalyst: (a) methanol/oil molar ratio, (b) catalyst dosage, (c) reaction temperature, and (d) reaction time.

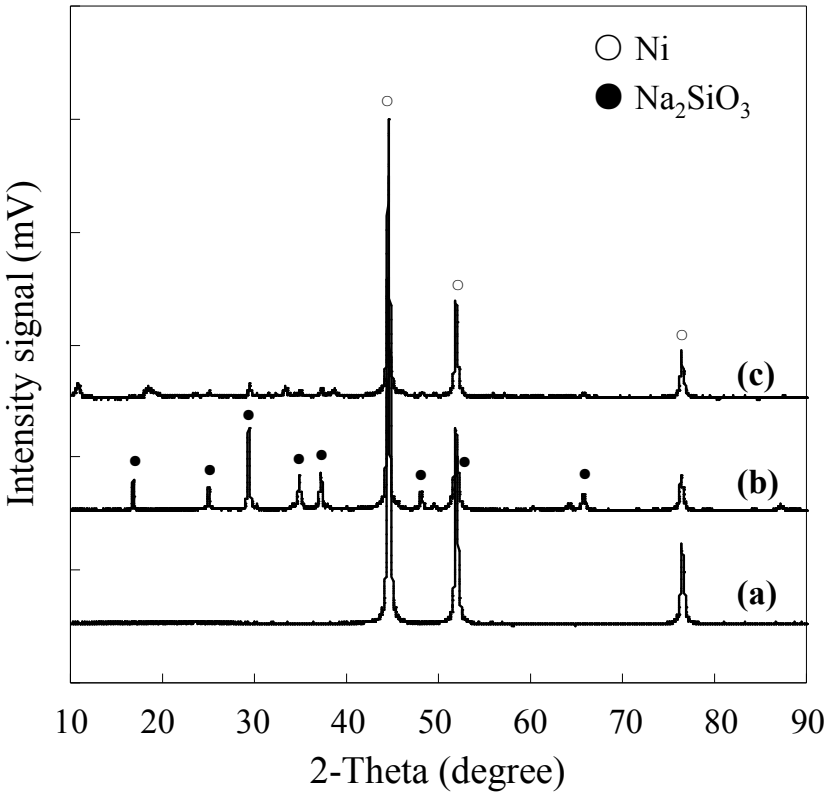

Fig. 3 XRD patterns of (a) Ni/C particles, (b) fresh and (c) deactivated Na_2SiO_3@Ni/C catalysts.

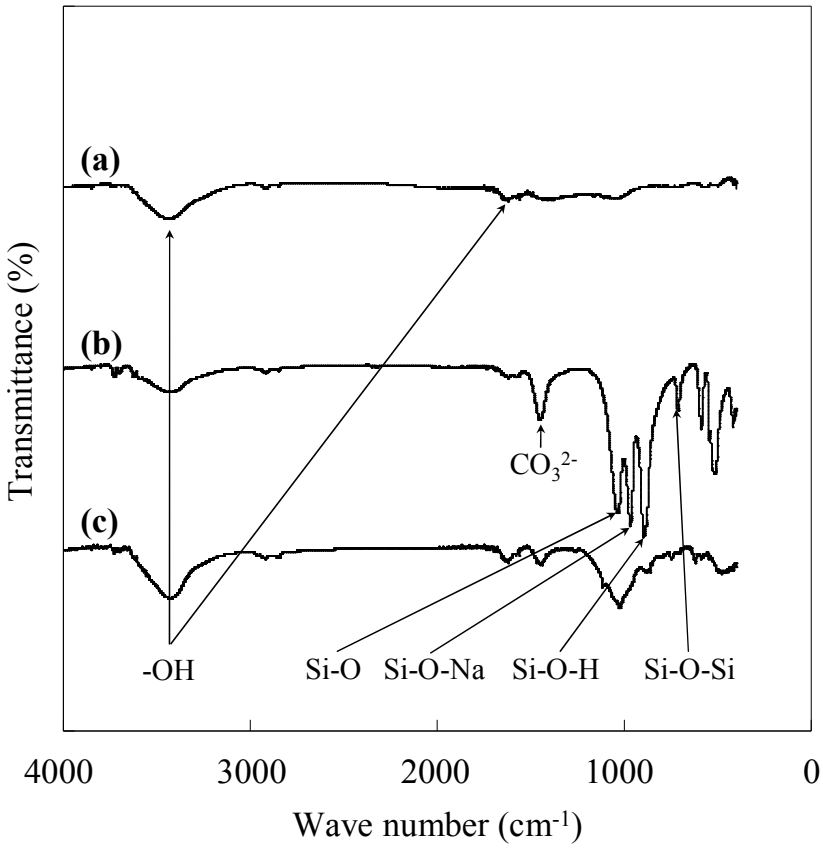

Fig. 4 FT-IR spectra of (a) Ni/C particles, (b) fresh and (c) deactivated Na_2SiO_3@Ni/C catalysts.

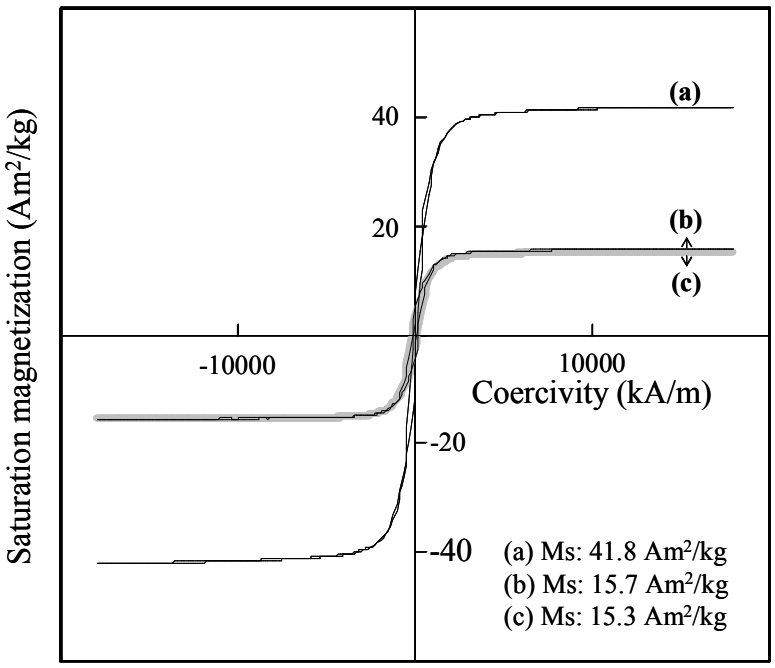

Fig. 5 Hysteresis loops of (a) Ni/C particles, (b) fresh and (c) deactivated Na_2SiO_3@Ni/C catalysts.

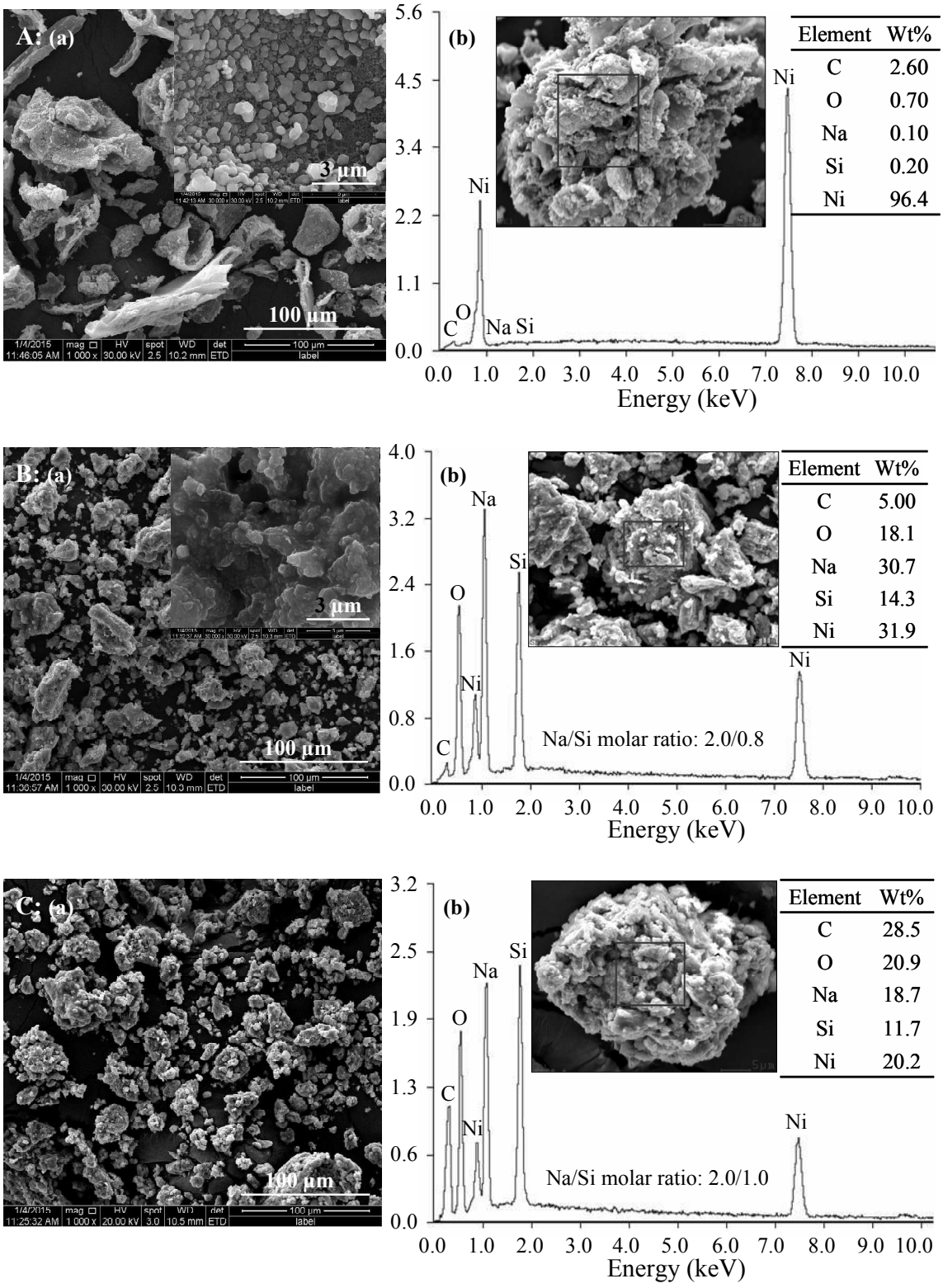

Fig. 6 (a) SEM images and (b) EDX spectra of (A) Ni/C particles, (B) fresh and (C) deactivated Na_2SiO_3@Ni/C catalysts (H is undetectable by EDX, and excluded in elemental composition).

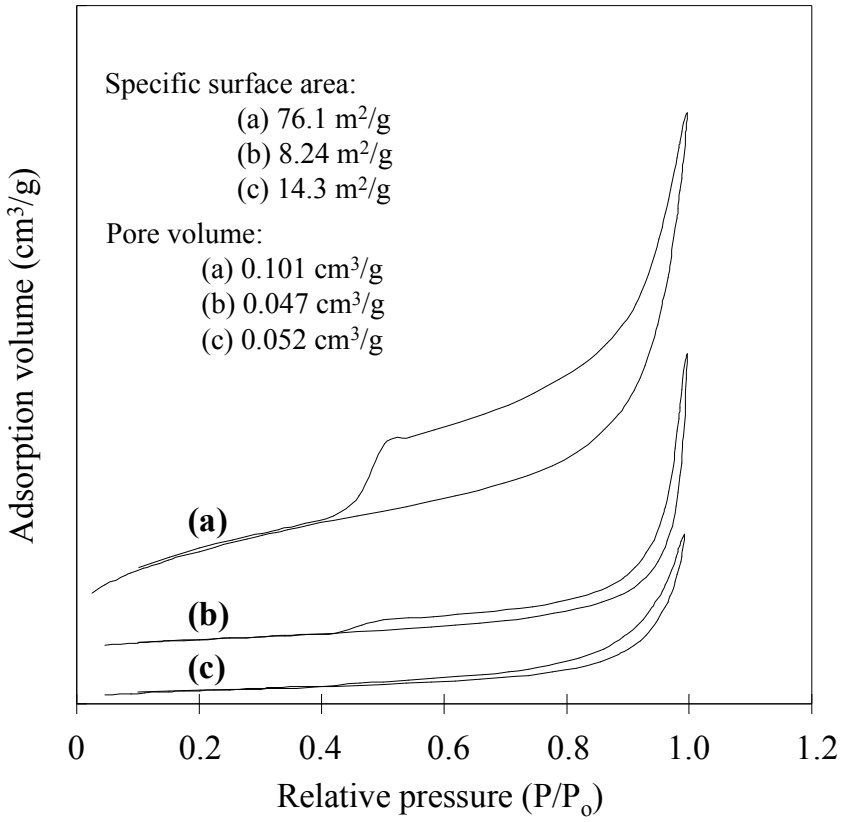

Fig. 7 Nitrogen adsorption/desorption isotherms of (a) Ni/C particles, (b) fresh and (c) deactivated Na_2SiO_3@Ni/C catalysts.

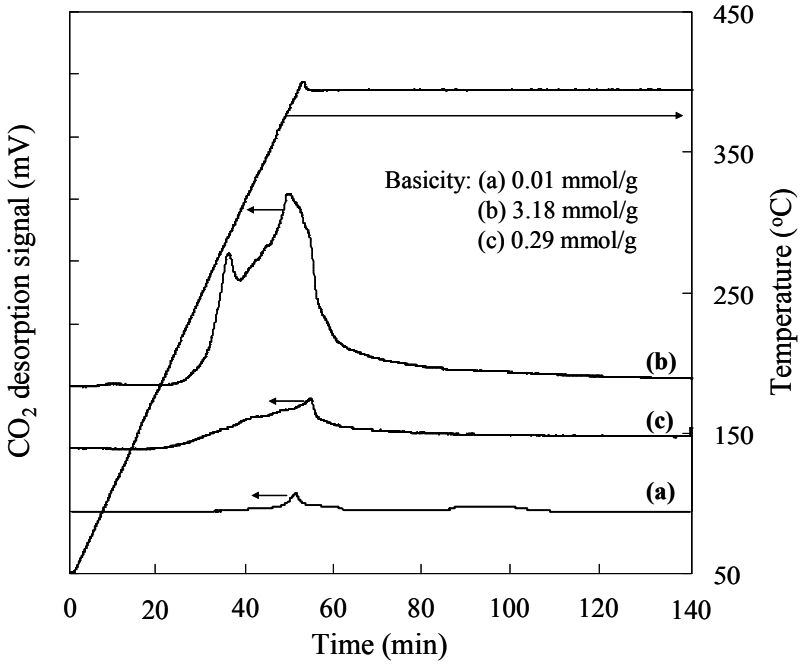

Fig. 8 CO_2-TPD profiles of (a) Ni/C particles, (b) fresh and (c) deactivated Na_2SiO_3@Ni/C catalysts.

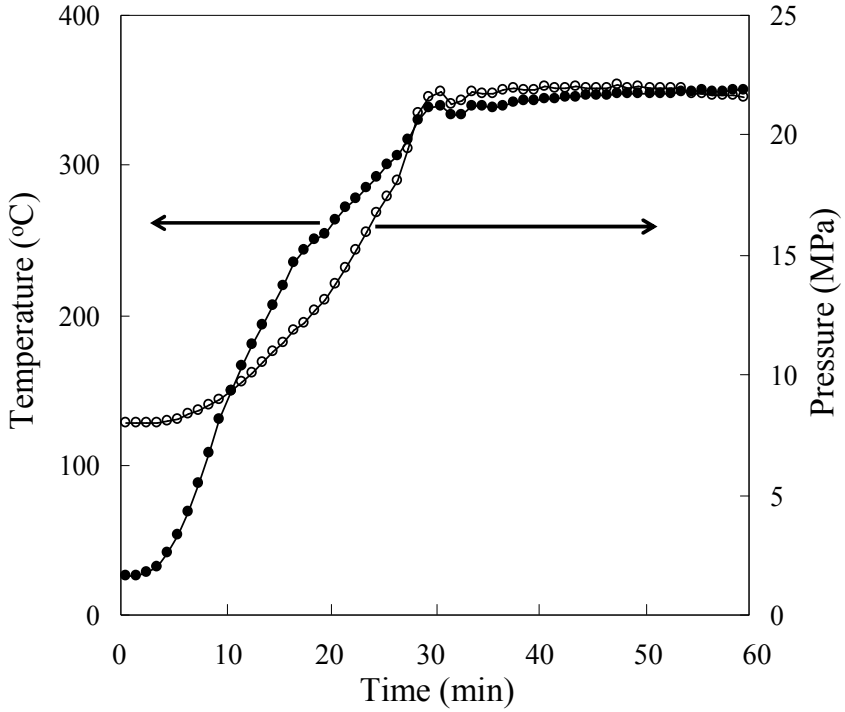

Fig. 9 Temperature and pressure versus time (0-60 min) in hydrothermal gasification of crude glycerol with deactivated Na_2SiO_3@Ni/C catalyst

[Experimental conditions: 0.46 g (total carbon 15 mmol) crude glycerol, 15 g H_2O, 55 min heating time from 20 to 350 ºC and 5 min holding time, 8.0 MPa initial pressure, 22.0 MPa highest reaction pressure.]

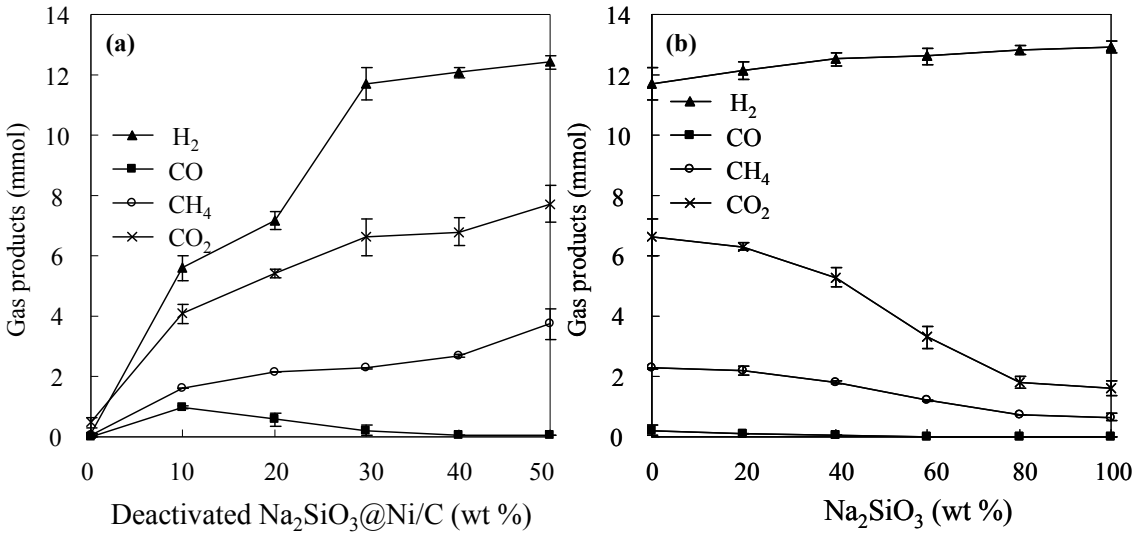

Fig. 10 Gas products from hydrothermal gasification of pure glycerol with various dosage of (a) deactivated Na_2SiO_3@Ni/C catalyst, and (b) Na_2SiO_3 with 30 wt% deactivated Na_2SiO_3@Ni/C catalyst.

[Experimental conditions: 0.46 g (total carbon 15 mmol) glycerol, 15 g H_2O, 55 min heating time from 20 to 350 ºC and 5 min holding time, 8.0 MPa initial pressure, 21.5-22.0 MPa highest reaction pressure.]

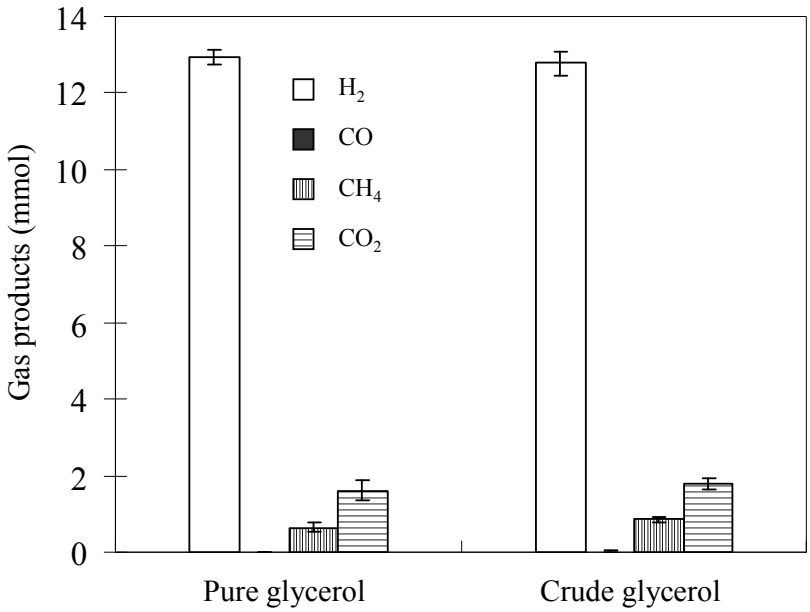

Fig. 11 Gas products from hydrothermal gasification of glycerol with 30 wt% deactivated Na_2SiO_3@Ni/C and 100 wt% Na_2SiO_3.
[Experimental conditions: 0.46 g (total carbon 15 mmol) glycerol, 15 g H_2O, 55 min heating time from 20 to 350 ºC and 5 min holding time, 8.0 MPa initial pressure, 22.0 MPa highest reaction pressure.]

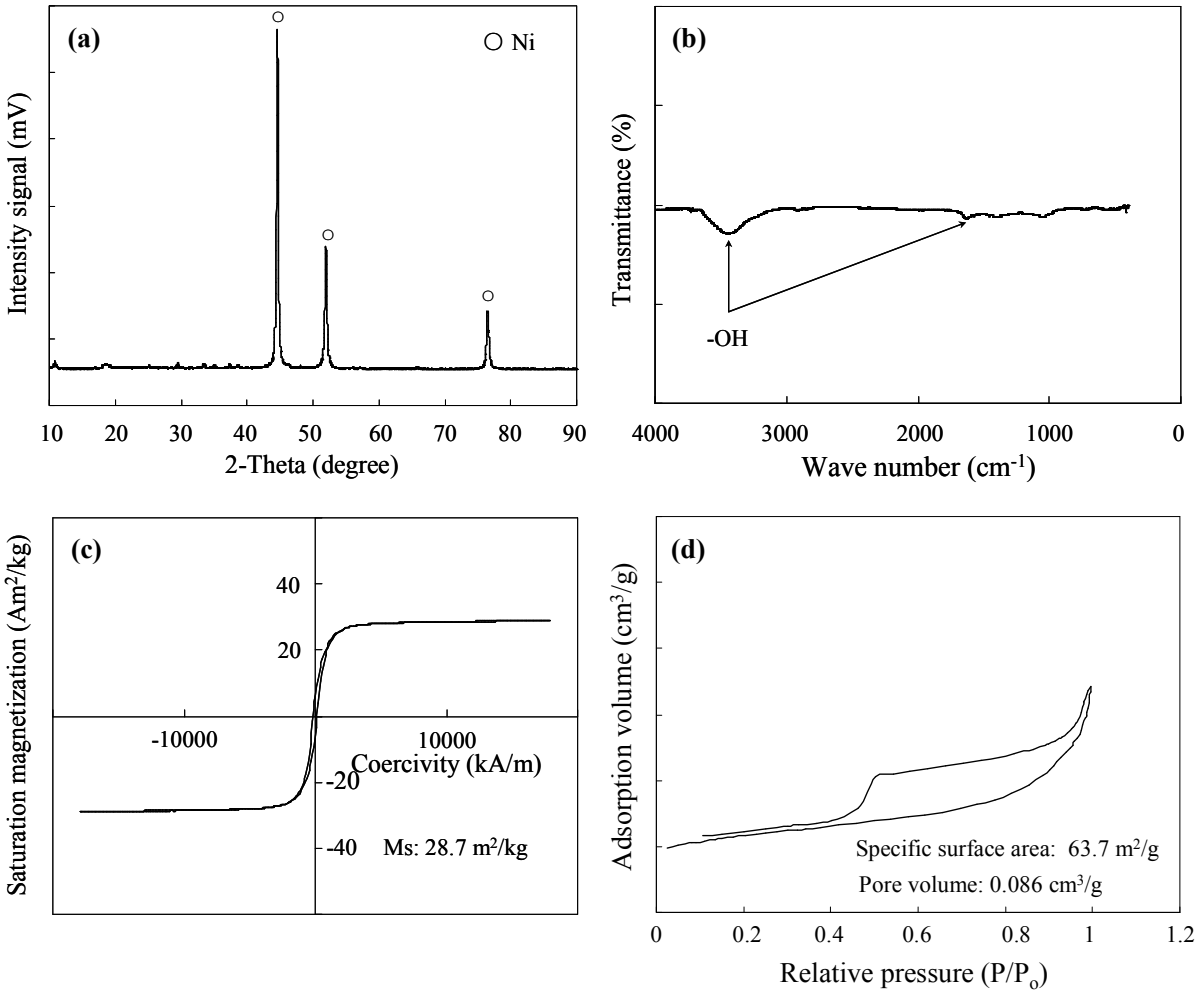

Fig. 12 Characterization of used deactivated Na_2SiO_3@Ni/C after gasification: (a) XRD, (b) FT-IR, (c) VSM, and (d) nitrogen adsorption/desorption isotherms.

Table of Contents:

Production of Biodiesel and Hydrogen from Plant Oil Catalyzed by Magnetic Carbon-Supported Nickel and Sodium Silicate

Authors: Fan Zhang, Xue-Hua Wu, Min Yao, Zhen Fang*, Yi-Tong Wang

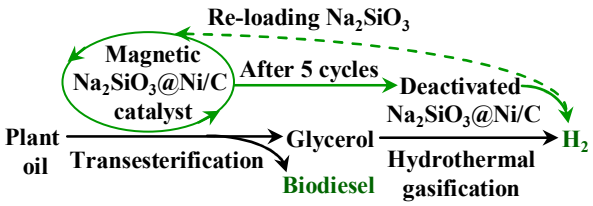

Production of biodiesel from plant oil catalyzed by magnetic Na_2SiO_3@Ni/C catalyst, and H_2 by the deactivated catalyst from by-product glycerol.